



Published in final edited form as:

J Am Chem Soc. 2013 September 4; 135(35): 12980–12983. doi:10.1021/ja406958k.

Cd²⁺ as a Ca²⁺ Surrogate in Protein–Membrane Interactions: Isostructural but Not Isofunctional

Krystal A. Morales^{†,‡}, Yuan Yang^{†,‡}, Zheng Long[†], Pingwei Li[†], Alexander B. Taylor[§], P. John Hart[§], and Tatyana I. Igumenova^{†,*}

[†]Department of Biochemistry and Biophysics, Texas A&M University, College Station, Texas 77843, United States

[§]Department of Biochemistry and the X-ray Crystallography Core Laboratory, University of Texas Health Science Center at San Antonio, San Antonio, Texas 78229, United States

Abstract

Due to its favorable spectroscopic properties, Cd²⁺ is frequently used as a probe of Ca²⁺ sites in proteins. We investigate the ability of Cd²⁺ to act as a structural and functional surrogate of Ca²⁺ in protein–membrane interactions. C2 domain from protein kinase C α (C2 α) was chosen as a paradigm for the Ca²⁺-dependent phosphatidylserine-binding peripheral membrane domains. We identified the Cd²⁺-binding sites of C2 α using NMR spectroscopy, determined the 1.6 Å crystal structure of Cd²⁺-bound C2 α , and characterized metal-ion-dependent interactions between C2 α and phospholipid membranes using fluorescence spectroscopy and ultracentrifugation experiments. We show that Cd²⁺ forms a tight complex with the membrane-binding loops of C2 α but is unable to support its membrane-binding function. This is in sharp contrast with Pb²⁺, which is almost as effective as Ca²⁺ in driving the C2 α -membrane association process. Our results provide the first direct evidence for the specific role of divalent metal ions in mediating protein–membrane interactions, have important implications for metal substitution studies in proteins, and illustrate the potential diversity of functional responses caused by toxic metal ions.

Ca²⁺-dependent signaling is involved in the regulation of many cellular processes, including those that occur at the membrane surfaces.^{1–3} The changes in intracellular Ca²⁺ levels are transduced to the membranes by two families of Ca²⁺ effector proteins: annexins^{4,5} and conserved homology-2 (C2) domains.^{6–8} Both are peripheral membrane proteins that undergo membrane association in Ca²⁺-dependent manner, with specificity toward negatively charged phospholipids, such as phosphatidylserine (PtdSer).^{9–11}

There are two views on the role of Ca²⁺ in mediating protein–membrane interactions. One view is that Ca²⁺ increases the electrostatic potential of the membrane-binding regions of the protein and thereby acts as a nonspecific “electrostatic switch”.¹² The other view is that

Corresponding Author: tigumenova@tamu.edu.

[‡]These authors contributed equally.

ASSOCIATED CONTENT

Supporting Information

Experimental details and crystallization data. This material is available free of charge via the Internet at <http://pubs.acs.org>.

The authors declare no competing financial interest.

Ca^{2+} specifically recognizes PtdSer headgroup through the formation of coordination bonds with the carboxyl and/or phosphoryl oxygens.^{13,14} The latter mechanism implies that the coordination sphere of protein-bound Ca^{2+} is dynamic: the labile water molecules coordinated by protein-bound Ca^{2+} are replaced by the lipid headgroup upon membrane association.

Due to its favorable spectroscopic properties (spin $I = 1/2$), $^{113}\text{Cd}^{2+}$ can potentially be used in lieu of Ca^{2+} to directly probe the changes in the metal coordination environment by NMR spectroscopy.¹⁵ In this work, we investigated the effect of Cd^{2+} on the structure and membrane-binding properties of the C2 domain from protein kinase C α (C2 α). Unexpectedly, we found that despite high affinity of Cd^{2+} to C2 α and the similar coordination geometry of protein-bound Cd^{2+} and Ca^{2+} , Cd^{2+} is unable to support the membrane-binding function of the protein. This is in sharp contrast with Pb^{2+} ions, whose coordination geometry in protein-bound state is different from that of Ca^{2+} , yet their ability to drive the C2 α -membrane association is comparable.¹⁶

Our findings shed light on the mechanism of metal-ion-dependent association of proteins with phospholipid membranes, illustrate how toxic metal ions can potentially interfere with Ca^{2+} signaling, and have important implications for designing metal substitution studies in proteins.

We used solution NMR to identify the Cd^{2+} binding sites in C2 α . The response of individual cross-peaks to increasing Cd^{2+} concentration was monitored in a series of ^{15}N - ^1H HSQC spectra. There are two groups of residues that respond differently to Cd^{2+} binding, as demonstrated for a selected subset in Figure 1. Group 1 falls into the slow-to-intermediate exchange regime on the NMR chemical-shift time scale, where the cross-peaks of the metal-complexed protein species appear at their final positions and gradually build up upon Cd^{2+} saturation. Group 2 shows fast-exchange behavior, where the cross-peak positions change smoothly in response to increasing Cd^{2+} concentration. These data indicate that there are two distinguishable types of Cd^{2+} binding sites in C2 α , with different binding kinetics of Cd^{2+} ions. The apparent Cd^{2+} affinities are also quite different, with groups 1 and 2 residues saturating at $\sim 300 \mu\text{M}$ and $\sim 4 \text{mM}$ Cd^{2+} , respectively.

To map the Cd^{2+} binding sites onto the structural elements of C2 α , we exploited their differential Cd^{2+} affinities and conducted the chemical shift perturbation (CSP) analysis for two pairs of Cd^{2+} concentration points: 0/240 and 240/4160 μM . Site 1 is mostly formed by the Ca^{2+} - and membrane-binding loops, or CMBLs (Figure 2A, shaded regions). According to the crystal structure of Ca^{2+} -complexed C2 α , CMBLs provide all ligands for the binuclear Ca^{2+} site. The CSP pattern in the low-concentration Cd^{2+} regime is very similar to that observed previously for the binding of two Ca^{2+} ions to C2 α .¹⁶ This suggests that no less than two Cd^{2+} ions with similar affinities bind to the loop region. We used the fluorescence emission spectra of native tryptophan residues in C2 α to estimate the affinity of Cd^{2+} to the high-affinity CMBL site. The shape of the binding curve indicates a significant degree of cooperativity (Figure 2B). The concentration of Cd^{2+} required to achieve half-maximal binding is $1.1 \pm 0.1 \mu\text{M}$. This value can be used as an upper limit for

the apparent dissociation constant K_d , given that the total concentration of C2 α is comparable (0.5 μ M).

The N-terminal/Helix3 region of C2 α forms the low-affinity Cd $^{2+}$ site (Figure 2A). This behavior is unique for Cd $^{2+}$, as the binding of Ca $^{2+}$ to this region of C2 α has not been observed. The Cd $^{2+}$ dissociation constant for this site can be estimated from the NMR data and is \sim 540 μ M (Figure 2C). Note that the separation of the Cd $^{2+}$ binding sites was possible due to the different total protein concentration regimes used for the fluorescence (0.5 μ M) and NMR (110 μ M) experiments.

To gain insight into the coordination geometry of protein-bound Cd $^{2+}$, we determined the crystal structure of the complex. The structure was refined to 1.60 \AA , with an R -free of 19.5%. Out of 6 Cd $^{2+}$ ions bound to C2 α , only 3 have 4 or more protein ligands: the binuclear Cd $^{2+}$ cluster in the CMBL region, with occupancies of 1.0 (Cd1) and 0.72 (Cd2); and Cd3 located between the N-terminal region and Helix3, with the occupancy of 0.4 (Figure 2D). The crystal structure of the complex is in good agreement with the NMR and fluorescence data: there are at least two CMBL Cd $^{2+}$ sites that are high-affinity (Figure 2B) and show intermediate-to-slow exchange regime with respect to Cd $^{2+}$ binding (Figure 2D, orange); and there is one Cd $^{2+}$ site that is low-affinity (Figure 2C) and shows fast exchange with respect to Cd $^{2+}$ binding (Figure 2D, blue). All details of fluorescence, NMR, and X-ray crystallography experiments are given in the SI, Sections 1–3.

The coordination geometry of CMBL-bound Cd $^{2+}$ is pentagonal bipyramidal and is very similar to that of Ca $^{2+}$ (Figure 3A and Table S3). The distance between the two metal ions is 3.7 and 3.8 \AA for Cd $^{2+}$ and Ca $^{2+}$, respectively. The protein ligands are: the carbonyl oxygens of W247 and M186 and the carboxyl oxygens of aspartate side chains in either bidentate (D187 and D248) or monodentate (D193, D246, and D254) coordination modes. The axial ligands of Cd1 and Cd2 sites are identical and include water molecules above and the carboxyl oxygens of the D246 side chain below the equatorial plane. Note that the Ca $^{2+}$ -complexed C2 α structure contains a short-chain PtdSer analog, whose phosphoryl oxygens serve as axial ligands of Ca1.

Two independent methods were used to quantify the metal-ion-dependent association of C2 α with membranes: protein-to-membrane FRET and lipid ultracentrifugation binding assays. FRET experiments relied on the native Trp residues and membrane-incorporated 1,2-dioleoyl-*sn*-glycero-3-phosphoethanolamine-*N*-(5-dimethylamino-1-naphthalenesulfonyl) (dansyl-PE) as donor and acceptor fluorophores, respectively.^{16,17} Titration of Ca $^{2+}$ into solution containing C2 α and large unilamellar vesicles (LUVs) comprising 1-palmitoyl-2-oleoyl-*sn*-glycero-3-phosphocholine/1-palmitoyl-2-oleoyl-*sn*-glycero-3-phospho-L-serine/dansyl-PE at a molar ratio of 73:20:7 resulted in the increase of dansyl fluorescence at 505 nm due to the protein-to-membrane FRET. In contrast, no changes in dansyl fluorescence were observed in the Cd $^{2+}$ titration experiments (Figure 3B). The absence of FRET cannot be attributed to the nonoptimal orientation of the transition dipoles because dansyl-PE is distributed randomly in the membrane. Cd $^{2+}$ alone neither quenches dansyl fluorescence nor associates appreciably with the PtdSer component of the LUVs under the conditions of our experiments (Figures S6 and S7). We conclude that Cd $^{2+}$ is unable to mediate the

association of C2 α with membranes. This was further demonstrated in the ultracentrifugation lipid-binding experiments, where the sucrose-loaded LUVs were incubated with C2 α and a solution of the corresponding metal ion and then pelleted by ultracentrifugation. The amount of protein left in the supernatant was quantified and used to calculate the fraction bound to the membranes. Addition of Ca²⁺ results in full membrane binding, while addition of Cd²⁺ does not (Figure 3C).

These findings are surprising in the context of our previous study on Pb²⁺ interactions with C2 α . In contrast to the structure of Ca²⁺-bound C2 α , M186 does not coordinate to Pb1 via the carbonyl oxygen; D246 and D254 serve as bidentate ligands to Pb1 and Pb2, respectively; and instead of pentagonal bipyramidal, Pb2 adopts hemidirected coordination geometry, with all eight ligands accommodated in one hemisphere (Figure 3D). Despite these differences, Pb²⁺ is almost as effective as Ca²⁺ in driving the protein–membrane interactions (Figure 3C and our previous work).¹⁶

We attribute this behavior to the coordination preferences of metal ions. Cd²⁺ is a soft Lewis acid,¹⁸ with preference toward soft ligands, such as thiol groups of cysteine residues.¹⁹ Its most frequently encountered coordination number (CN) in proteins is either 4 or 6.²⁰ The crystal structures of Ca²⁺-bound C2 α ¹³ and annexin V¹⁴ in complex with PtdSer analogs suggest that a Ca²⁺-coordinated water molecule is replaced by either phosphoryl and/or carboxyl oxygen(s) of PtdSer upon membrane association. This may be accompanied by an expansion of the metal ion coordination sphere, as shown for Ca²⁺-bound C2 α in Figure 3A. While Cd²⁺ can adopt a hepta-coordinated state when bound to C2 α , the rearrangement and possible expansion of its all-oxygen coordination sphere required for PtdSer interactions may be unfavorable. In contrast, Ca²⁺ is a hard Lewis acid that favors all-oxygen coordination environment with CNs of 6–8.²¹ Pb²⁺ is a borderline Lewis acid that interacts readily with oxygen-containing ligands and can adopt CNs up to 9 in proteins.²²

To test if the ability of a metal ion to expand the coordination sphere is important for membrane binding, we characterized the interactions of C2 α with Cu²⁺. Similar to Pb²⁺, Cu²⁺ is a borderline Lewis acid, albeit with a well-documented preference for CN = 4 in proteins.²⁰ In addition, Cd²⁺ and Cu²⁺ have been used with success as a diamagnetic–paramagnetic pair in structural studies.²³ In the presence of 50 μ M Cu²⁺, cross-peaks of C2 α residues in the N-terminal/Helix3 region broaden beyond detection due to the paramagnetic relaxation enhancement (PRE) caused by bound Cu²⁺ (Figure 4A). Increasing the concentration of Cu²⁺ to 150 μ M results in efficient relaxation of all CMBL regions. These data suggest that Cu²⁺ populates the same set of C2 α sites as Cd²⁺, albeit with the opposite pattern of affinities (Figures S8 and S9). The lipid-binding assays show that like Cd²⁺, Cu²⁺ is not an effective mediator of protein–membrane interactions: only ~30% of Cu²⁺-complexed C2 α is membrane bound (Figure 3C). Reducing the concentration of PtdSer from 30% to 20% eliminates the membrane binding of C2 α in the presence of Cu²⁺ (Figure S10).

We carried out Ca²⁺/Cu²⁺ displacement experiments to assess the role of the N-terminal/Helix3 metal ion-binding site in protein–membrane interactions. In the membrane-free environment, the cross-peaks of CMBL residues that are broadened beyond detection in the presence of the 250 μ M Cu²⁺ are recovered upon addition of 3.0 mM Ca²⁺ (Figure 4B,C). In

contrast, the resonances in the vicinity of the N-terminal/Helix3 site remain broadened due to the presence of bound Cu^{2+} . These data indicate the formation of mixed metal-ion species, with Ca^{2+} and Cu^{2+} bound to the CMBL and N-terminal/Helix3 regions of C2 α , respectively. The ability of this species to associate with PtdSer-containing membranes was tested in ultracentrifugation lipid-binding experiments for two concentration regimes, with full membrane binding observed in both cases (Figure 3C, bars 1 and 2). Thus, having a divalent metal ion bound to the N-terminal/Helix3 site does not negatively affect the C2 α membrane-binding properties.

Taken together, our findings support the view that a divalent metal ion plays a specific role in mediating protein–membrane interactions, rather than the nonspecific “electrostatic switch” model. All three non-native metal ions: Cd^{2+} , Cu^{2+} , and Pb^{2+} can increase the electrostatic potential of C2 α through direct binding to the aspartate-rich CMBL region. However, the formation of metal ion-protein complex is not sufficient to promote protein–membrane association, as demonstrated for Cd^{2+} and Cu^{2+} . We conclude that specific interactions of a divalent metal ion with PtdSer group(s) are required for productive protein–membrane interactions.

Favorable spectroscopic properties and the nearly identical ionic radius have made Cd^{2+} a popular substitute for Ca^{2+} .¹⁵ Our results show that the preferred coordination geometry of metal ions, their ability to expand the coordination sphere, and the chemical identity of protein ligands need to be taken into account when designing metal substitution studies. This is particularly important for proteins that rely on metal ions to carry out a specific function. A case in point is the C2 domains, which are the second most abundant lipid-binding domain behind the PH:²⁴ a UniProt²⁵ search produced >140 different human C2-containing proteins whose function includes signal transduction and membrane trafficking.

Cd^{2+} is a toxic metal ion with no safe limit of exposure.²⁶ In our study, the affinity of Cd^{2+} to the CMBL region exceeds the previously reported Ca^{2+} value²⁷ >30-fold. It is plausible that bioavailable Cd^{2+} can influence the function of C2-domain containing proteins through a direct competition with Ca^{2+} for the CMBL regions. Our results demonstrate that toxic metal ions, such as Cd^{2+} and Pb^{2+} , can elicit very different functional responses with respect to the *in vitro* membrane binding: Pb^{2+} promotes membrane association of C2 α , whereas Cd^{2+} does not. Either scenario, if occurring in the cell, would lead to the aberration in the Ca^{2+} signaling response.

Supplementary Material

Refer to Web version on PubMed Central for supplementary material.

Acknowledgments

This work was supported in part by the NSF CAREER (CHE-1151435) and Welch Research Foundation (A-1784) awards to T.I.I.

REFERENCES

1. Berridge MJ, Lipp P, Bootman MD. Nat. Rev. Mol. Cell Biol. 2000; 1:11. [PubMed: 11413485]

2. Clapham DE. *Cell*. 2007; 131:1047. [PubMed: 18083096]
3. Patergnani S, Suski JM, Agnoletto C, Bononi A, Bonora M, De Marchi E, Giorgi C, Marchi S, Missiroli S, Poletti F, Rimessi A, Duszynski J, Wieckowski MR, Pinton P. *Cell Commun. Signaling*. 2011; 9:19.
4. Lizarbe MA, Barrasa JI, Olmo N, Gavilanes F, Turnay J. *Int. J. Mol. Sci.* 2013; 14:2652. [PubMed: 23358253]
5. Gerke V, Creutz CE, Moss SE. *Nat. Rev. Mol. Cell Biol.* 2005; 6:449. [PubMed: 15928709]
6. Nalefski EA, Falke JJ. *Protein Sci.* 1996; 5:2375. [PubMed: 8976547]
7. Rizo J, Sudhof TC. *J. Biol. Chem.* 1998; 273:15879. [PubMed: 9632630]
8. Corbalán-García S, Gómez-Fernández JC. *BioFactors*. 2010; 36:1. [PubMed: 20049899]
9. Richter RP, Him JL, Tessier B, Tessier C, Brisson AR. *Biophys. J.* 2005; 89:3372. [PubMed: 16085777]
10. Vats K, Knutson K, Hinderliter A, Sheets ED. *ACS Chem. Biol.* 2010; 5:393. [PubMed: 20175560]
11. Stahelin RV, Rafter JD, Das S, Cho W. *J. Biol. Chem.* 2003; 278:12452. [PubMed: 12531893]
12. Murray D, Honig B. *Mol. Cell.* 2002; 9:145. [PubMed: 11804593]
13. Verdaguer N, Corbalán-García S, Ochoa WF, Fita I, Gómez-Fernández JC. *EMBO J.* 1999; 18:6329. [PubMed: 10562545]
14. Swairjo MA, Concha NO, Kaetzel MA, Dedman JR, Seaton BA. *Nat. Struct. Biol.* 1995; 2:968. [PubMed: 7583670]
15. Armitage IM, Drakenberg T, Reilly B. *Met. Ions Life Sci.* 2013; 11:117. [PubMed: 23430773]
16. Morales KA, Lasagna M, Gribenko AV, Yoon Y, Reinhart GD, Lee JC, Cho W, Li P, Igumenova TI. *J. Am. Chem. Soc.* 2011; 133:10599. [PubMed: 21615172]
17. Nalefski EA, Falke JJ. *Methods Mol. Biol.* 2002; 172:295. [PubMed: 11833355]
18. Pearson RG. *J. Am. Chem. Soc.* 1963; 85:3533.
19. Chakraborty S, Kravitz JY, Thulstrup PW, Hemmingsen L, DeGrado WF, Pecoraro VL. *Angew. Chem., Int. Ed. Engl.* 2011; 50:2049. [PubMed: 21344549]
20. Rulíšek L, Vondrášek J. *J. Inorg. Biochem.* 1998; 71:115. [PubMed: 9833317]
21. Kirberger M, Wang X, Deng H, Yang W, Chen G, Yang JJ. *J. Biol. Inorg. Chem.* 2008; 13:1169. [PubMed: 18594878]
22. Kirberger M, Yang JJ. *J. Inorg. Biochem.* 2008; 102:1901. [PubMed: 18684507]
23. Jensen MR, Hansen DF, Ayna U, Dagil R, Hass MAS, Christensen HEM, Led JJ. *Magn. Reson. Chem.* 2006; 44:294. [PubMed: 16477687]
24. Cho W, Stahelin RV. *Biochim. Biophys. Acta, Mol. Cell Biol. Lipids.* 2006; 1761:838.
25. UniProt Consortium. *Nucleic Acids Res.* 2012; 40:D71. [PubMed: 22102590]
26. Thévenod F, Lee WK. *Met. Ions Life Sci.* 2013; 11:415. [PubMed: 23430781]
27. Kohout SC, Corbalán-García S, Torrecillas A, Gómez-Fernández JC, Falke JJ. *Biochemistry.* 2002; 41:11411. [PubMed: 12234184]

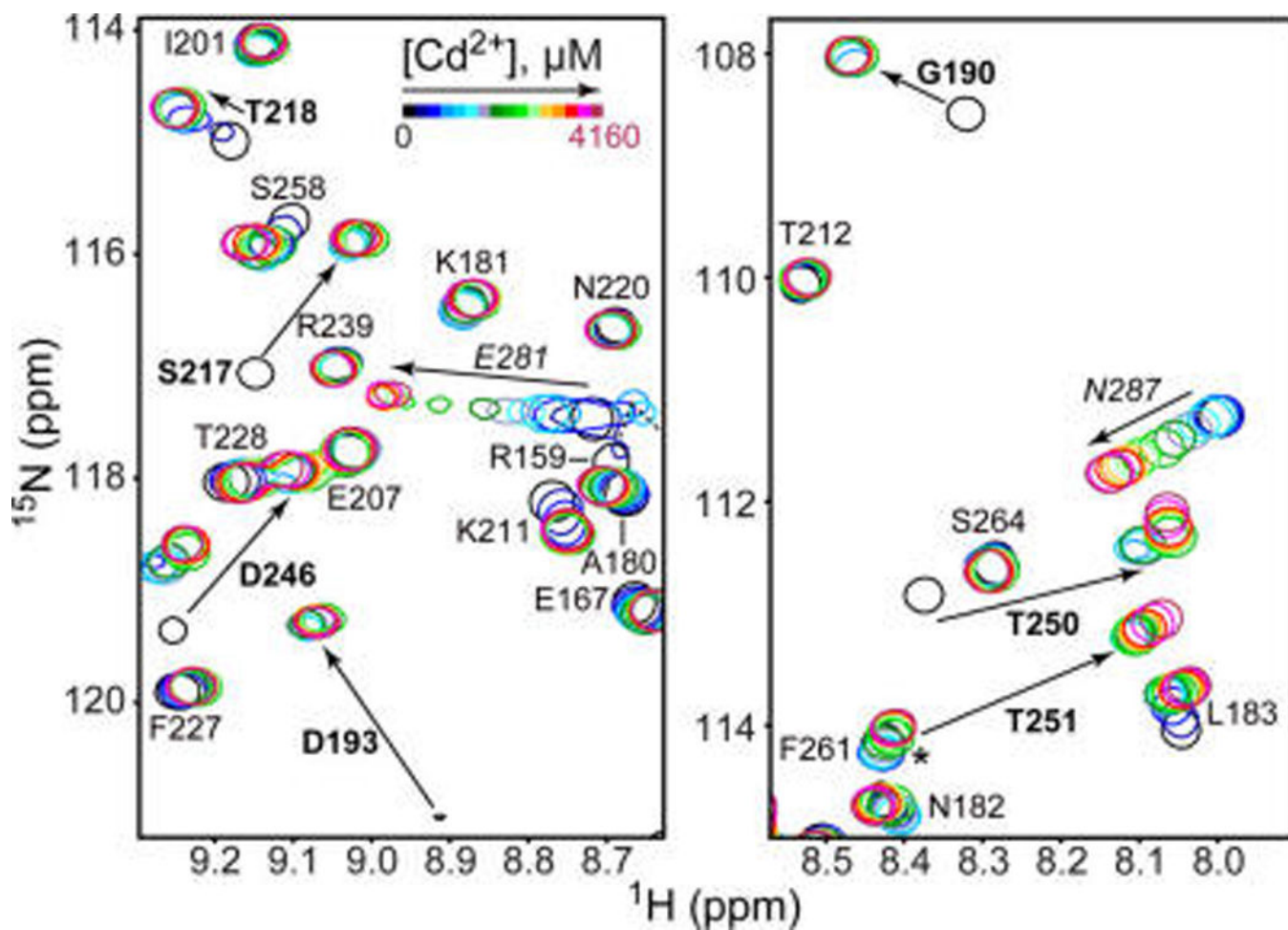


Figure 1.

Two types of Cd^{2+} binding sites in C2 α . Expansions of the ^{15}N - ^1H HSQC spectra showing the chemical shift changes of 110 μM C2 α in response to increasing Cd^{2+} concentration.

Residues of groups 1 and 2 are shown in boldface and italics, respectively. Asterisk marks the position of the apo C2 α T251 cross peak, which overlaps with F261.

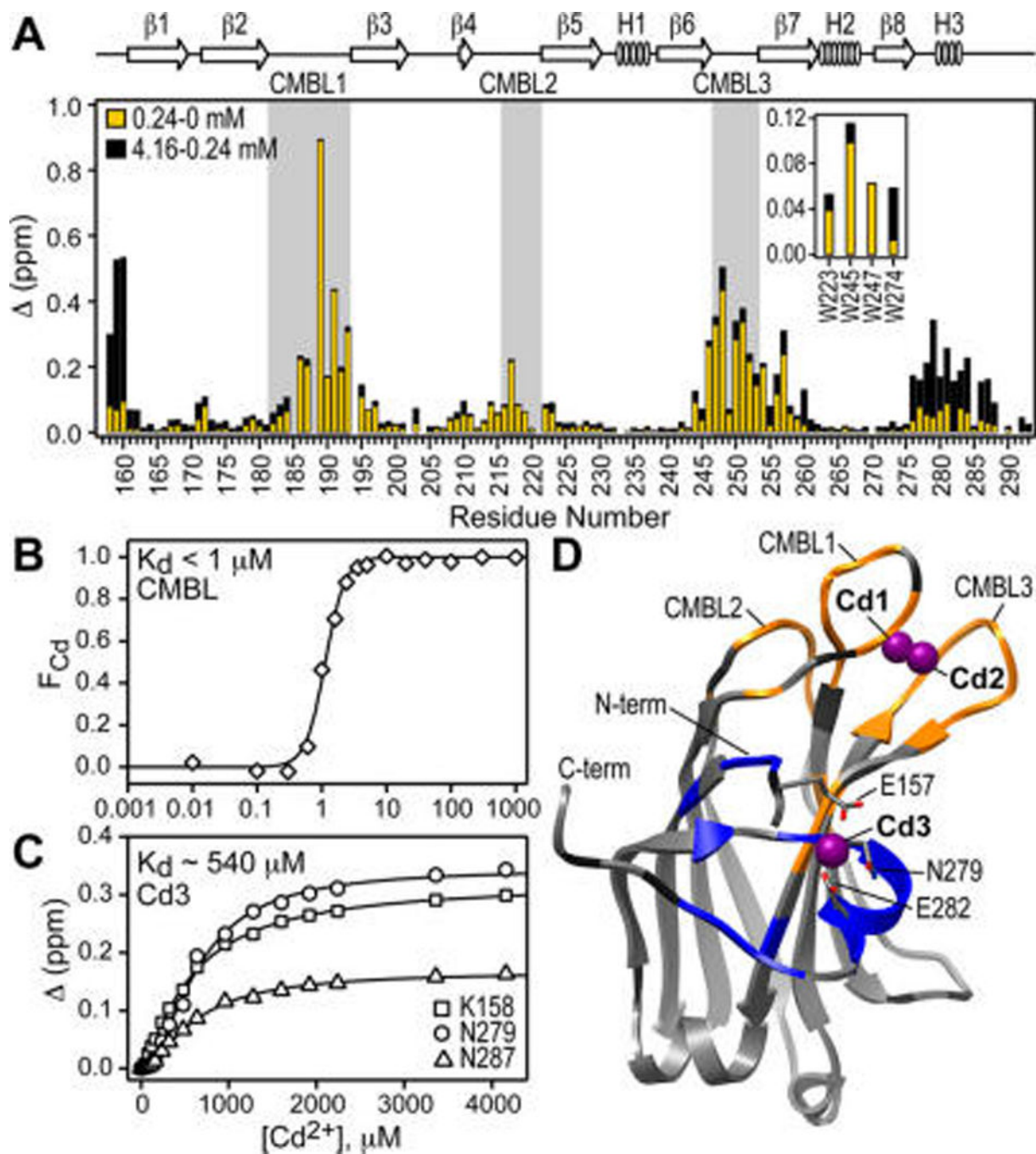


Figure 2. Cd^{2+} binds to two distinct C2 α regions: CMBLs and N-terminal/Helix3 region. (A) Chemical shift perturbation for low- (yellow) and high-concentration (black) Cd^{2+} regimes, demonstrating the presence of two types of sites. Inset shows Δ values for the indole N-H groups of Trp side chains. (B) Fraction of the Cd^{2+} -complexed C2 α , F_{Cd} , calculated using the change in the spectral center of mass of the Trp fluorescence emission spectra, plotted against Cd^{2+} concentration. (C) Representative NMR-detected Cd^{2+} binding curves for N-terminal/Helix3 region. (D) Crystal structure of the Cd^{2+} -complexed C2 α .

(PDB ID 4L1L). Residues showing intermediate-to-slow and fast exchange regimes upon Cd^{2+} binding are highlighted in orange and blue, respectively. Pro and residues with no data are dark gray.

Author Manuscript

Author Manuscript

Author Manuscript

Author Manuscript

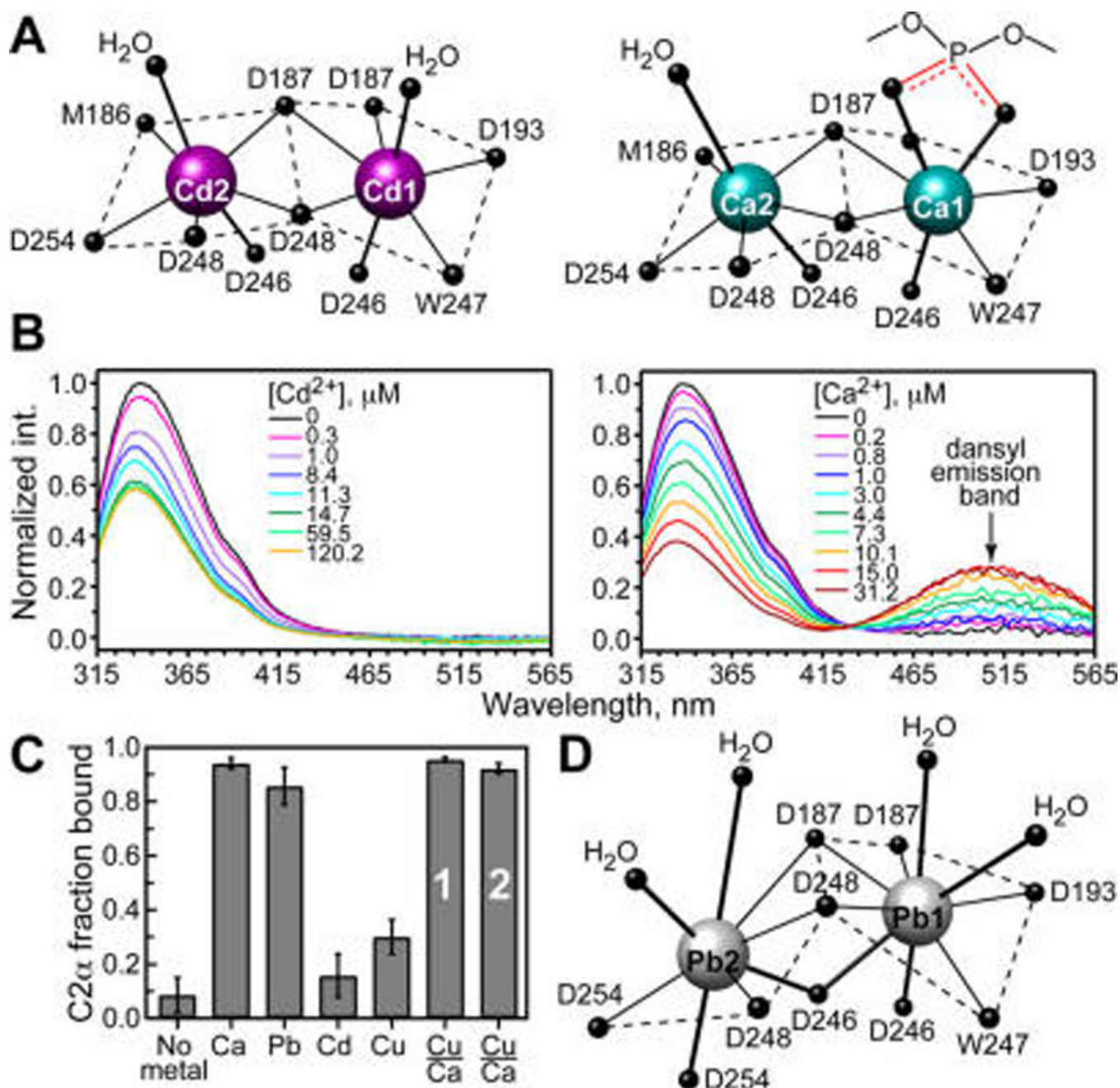


Figure 3. Coordination geometry of metal ions does not correlate with their ability to mediate C2 α -membrane association. (A) Coordination geometry of CMBL-bound Cd²⁺ (4L1L) and Ca²⁺ (1DSY).¹³ (B) Fluorescence emission spectra, obtained as the difference between the spectra of C2 α -containing and C2 α -free dansyl-doped LUVs. Build-up of the dansyl band in Ca²⁺ experiments is due to protein–membrane FRET. (C) Fractional population of membrane-bound C2 α obtained in ultracentrifugation binding assays with LUVs having 30% PtdSer component. Total concentration of metal ions was 175 μ M, except for the Cu²⁺/Ca²⁺

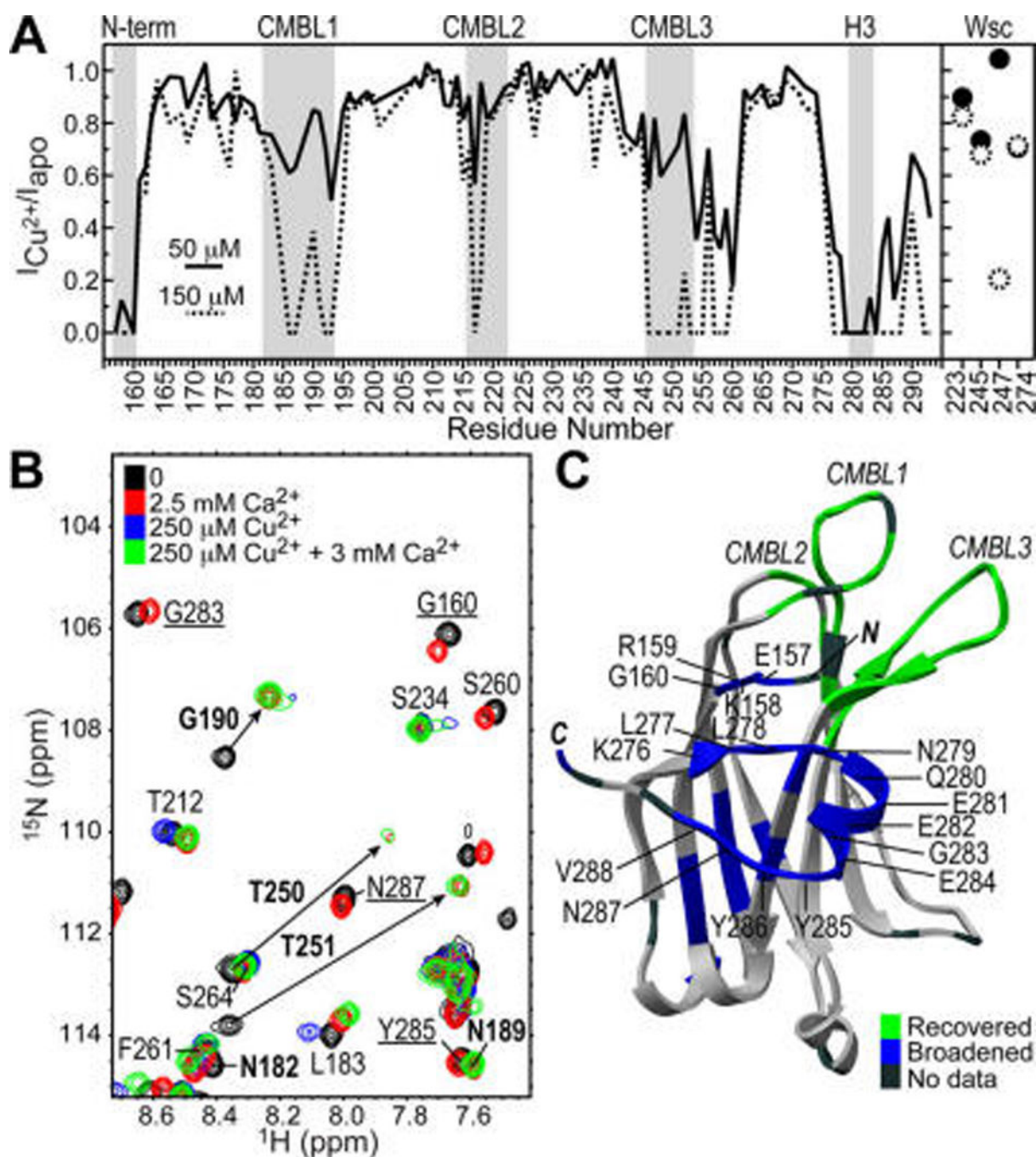
displacement experiments that were carried out at 12.5/175 μM (bar 1) and 175/2450 μM (bar 2). (D) Coordination geometry of CMBL-bound Pb^{2+} (3TWY).¹⁶

Author Manuscript

Author Manuscript

Author Manuscript

Author Manuscript

**Figure 4.**

Ca^{2+} displaces Cu^{2+} from the CMBL region of C2a, with formation of mixed Ca^{2+}/Cu^{2+} -bound species. (A) PRE, calculated as ratio of NMR cross-peak intensities in Cu^{2+} -bound C2a to those in apo C2a, for two Cu^{2+} concentrations: 50 and 150 μ M. Data were normalized to residue K236. (B) Overlay of ^{15}N - 1H HSQC spectra of 100 μ M C2a at several concentrations of Ca^{2+} and Cu^{2+} . Residues that remain broadened upon addition of 12-fold Ca^{2+} excess over Cu^{2+} are underlined. Residues whose intensity fully recovers upon addition of Ca^{2+} are shown in boldface. Arrows indicate direction of cross-peaks' shift due

to Ca²⁺ binding. (C) Mapping of broadened residues (blue) and residues recovered upon Ca²⁺ addition (green) onto the structure of apo C2a (3RDJ).¹⁶

Author Manuscript

Author Manuscript

Author Manuscript

Author Manuscript